

# Use Of Rice Straw As Biosorbent For Removal Of Co(II) Ions From Synthetic Waste Water

A.A. Swelam<sup>1</sup>, M.B. Awad<sup>1</sup>, A.M.A. Salem<sup>1</sup> and A.S. El-Feky<sup>1</sup>

<sup>1</sup> Chemistry Department, Faculty of Science, Al-Azhar University Cairo, Egypt

## Abstract

The current study explains the effect of acid pretreatments on rice straw (MRS) for the removal of Co(II) from aqueous solution. MRS showed improvement in adsorption capacity. The kinetic data were analyzed in term of pseudo first-order, pseudo second-order and intraparticle diffusion expressions. It is found that the pseudo second-order model was the best model for the adsorption process. The Langmuir, Freundlich, D-R and Temkin isotherm models were applied to the equilibrium data and defined very well the Langmuir isotherm model. The results show that, the mean values of the thermodynamic parameters of activation energy ( $E_a = 8.33 \text{ kJ mol}^{-1}$ ), the sticking factor ( $S^* \leq 1$ ), standard free energy ( $\Delta G^0 = -8.6 \text{ kJ mol}^{-1}$ ), standard enthalpy ( $\Delta H^0 = 12.45 \text{ kJ mol}^{-1}$ ) and standard entropy ( $\Delta S^0 = 28.53 \text{ mol}^{-1} \text{ K}^{-1}$ ) of the adsorption mechanism were determined.

**Key words:** Rice straw, removal, Cobalt, Kinetic, Thermodynamic

## 1. Introduction

The removal and recovery of toxic metal ions from wastewater have become important research areas in terms of environmental issues, and widely been studied from various aspects in recent years. A number of approaches such as ion exchange, adsorption, chemical precipitation, reverse osmosis and electro dialysis techniques have been developed for this purpose. Synthetic resins having the functionalities to form chelate structures are also candidate compounds for the removal and recovery of toxic metal ions in wastewater. However, in the case of petroleum-based synthetic polymers, suitable post treatments of the used resins containing metal ions are required, and it may cause secondary pollution during the post treatments. Moreover, most petroleum-based synthetic polymers are neither renewable nor biodegradable.

On the other hand, cellulose is the most abundant and renewable biopolymers, and is one of the promising raw materials available in terms of cost for the preparation of various functional materials. However, because native cellulosic fibers generally have quite low carboxyl and other functional groups, they have no or nearly no metal-anchoring capability per se. Hence, many attempts have been made to utilize cellulose as a metal scavenger through some derivatizations.

Several pretreatment methods have been used to break the biological barriers to produce cellulosic ethanol, such as dilute acid [1], steam explosion [2] and lime [3]. These methods are based on principle of partial hydrolysis of the hemicellulose acetyl group, redistribution or cleavage of lignin, which has been proven to be effective in increasing the cellulose hydrolysis. Alkaline solution has advantages of removal of lignin, but it suffers from dealing with sustained pollutant and following up management cost.

The hot acid solution is the most popular pretreatment method of straw, by which the amorphous hemicellulose and/or lignin is easily removed by  $H^+$  and hemicellulose will be partial hydrolyzed to mono- and oligosaccharides. Furthermore, both morphological and structural characteristics are changed due to organic polar substances and inorganic silica partly dissolved and leaving of the high surface area with a more mesoporous pore on acid-treated plant residue. Increasing of crystallinity and exposed cellulose having bigger microcrystalline size are helpful to produce fermentable ethanol by removal of amorphous component such as hemicellulose/lignin and accompanied by breaking of hydrogen bonding within inter-microfibril [4].

The content of lignin in rice straw is less than in other common feedstocks, such as corn stover and wheat straw. Therefore, the effect of lignin composition on the enzymatic hydrolysis of rice straw may be different from another that which occurs in the other biomass materials. Moreover, the hemicelluloses–lignin matrix that surrounds the cellulose fraction in the biomass has been suggested to act as a physical barrier, which hinders the access of cellulase to the surface of the cellulose. It is believed that removing the hemicellulose may increase the pore volume and surface area of the solid residue and assist access of cellulose to the cellulose structure [5].

In addition, the cellulase attack generally prefers to occur in an amorphous region of the cellulose. Thus, the solid residues with high crystalline structure probably give fewer attack sites at which cellulase initiate the hydrolytic reaction [5]. For corn stover with dilute acid pretreatment, it was found that the level of crystallinity of the pretreated solid residues had a negative effect on the initial rate of hydrolysis. Thus, the enzymatic hydrolysis of lignocellulosic materials are a complicated reaction due to the heterogeneous structural properties of the raw materials. The effect of degree of crystallinity of the pretreated rice straw on enzymatic hydrolysis is still not understood [6].

The aim of this study was to identify the reasonable conditions for the dilute acid pretreatment of rice straw, which was evaluated by estimating the cobalt removal from aqueous solution. In addition, structural features of the pretreated rice straw were also investigated by analyzing crystallinity and the FTIR spectrum in order to clarify the effects of the acid-catalyzed reaction of adsorption capacity. Furthermore, a comprehensive comparison of raw rice straw and pretreated rice straw was also made in order to evaluate the potential of dilute acid pretreatment in the cobalt uptake.

## **2. Materials and methods**

### **2.1. Materials**

The rice straw (RS) used as raw material was obtained from Menofia, Egypt. Hydrochloric acid (35% purity) was used for acid treatment. Hydrochloric acid was used for hydrolysis. All chemicals were purchased from System Chem AR and Sigma–Aldrich and were used without further purification.

### **2.2. Acid hydrolysis**

The acid hydrolysis treatment was conducted on the raw rice straw treatment at a temperature of 28 °C using 0.1 M of hydrochloric acid (pre-heated) for 24h under continuous stirring. The hydrolysed material was washed by centrifugation at 10,000 rpm at 28°C for 10 min. This centrifugation step was repeated several times before the suspension was dialysed against distilled water for several days until constant pH in the range of  $\approx 7$  was reached. The resulting suspension (MRS) was then kept in desiccator for used.

### 2.3. Preparation of metal-solutions

The Co(II) stock solution containing 1000 mg/L was prepared by dissolving cobalt chloride (analytical reagent grade) in distilled water. Cobalt working solutions in different concentrations was prepared by diluting the Co (II) stock solution with distilled water.

### 2.4. Analytical technique

The concentrations of the Co (II) metal ions were performed using Flame Atomic Absorption Spectrophotometer (FAAS) Vario 6. Elements were determined using an air– acetylene flame.

## 3. Discussion and results

### 3.1. Characterization of adsorbents

#### 3.1.1. Chemical composition of RS and MRS

The chemical composition of the RS and MRS was determined and the data are summarized in Table 1.

Table 1 : Chemical Characterization of RS and MRS.

No.	Chemical Characterization	Samples	
		RS	MRS
1	Moisture Content %	7	6.27
2	Ash Content %	6	9.5
3	Lignin Content %	12.5	13.8
4	Holocellulose %	75.5	82.9
5	Alpha Cellulose	56	56.7

#### 3.1.2. Spectroscopic analysis (FTIR)

The spectra of RS and MRS were measured within the range of 400–4000  $\text{cm}^{-1}$  wave number. As shown in Fig. 1.a and fig.1.b Significant changes of the functional group were visible after acid treatment. Acid treatment (HCl) was used for cleaning the cell wall and replacing the natural mix of ionic species bound on the cell wall with protons. The acid hydrolysis convert amide and ester groups to corresponding carboxylic acids. A broad band in the region  $\sim 3430 \text{ cm}^{-1}$  in spectra may be assigned to -OH stretching vibrations mode of hydroxyl functional groups including hydrogen bonding of chemisorbed water or may be due to binding of -OH group with polymeric structure of MRS. A new

peak emerged at  $\sim 2923\text{cm}^{-1}$  in spectrum of MRS, which is not so prominent in spectrum of raw rice straw, may be attributed to C-H stretching of aliphatic carbon or can be due to  $-\text{CH}_2$  or  $-\text{CH}_3$  deformation. The increased sorption potential of MRS as compared to untreated may be due to formation of these stretching bands. Peak obtained at  $\sim 1641\text{ cm}^{-1}$  may be due to olefinic C=C and carbonyl C=O stretching frequencies of hemicellulose, lignin and amino groups. This peak became more prominent in MRS, justifying its higher sorption potential due to this structural modification. The observed peak in the spectra of  $1523\text{ cm}^{-1}$  [7,8] is attributed to ether and carboxylate groups.

To confirm the difference in functional groups after the biosorption of Co(II), FTIR study was carried out using Co(II) loaded MRS. The absorption spectrum of cobalt-loaded adsorbent was compared with that of unloaded MRS. A change of absorption bands can be seen when comparing the FTIR spectra of pristine and cobalt-loaded biomass (Fig. 1.a and 1.b). This figure also shows the changes in the spectrum of the biosorbent after sorption of Co(II). An interesting phenomenon was the disappearance of the band intensity at 1459 and  $1259\text{ cm}^{-1}$  after metal binding. Although, slight changes in other absorption frequencies were observed, it was difficult to interpret how these absorption peaks were related with Co(II) biosorption [9].

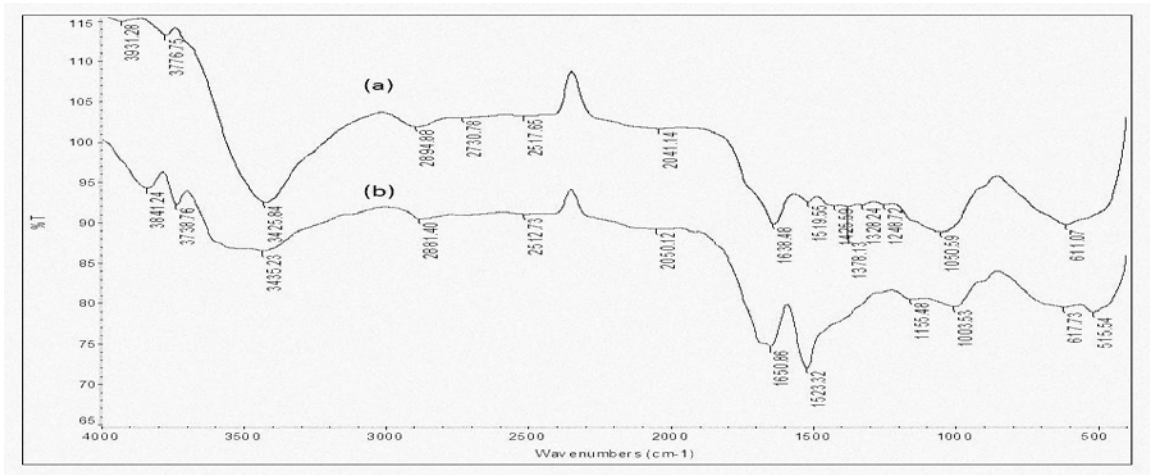


Fig. 1.a. FTIR spectra for RS (a) before and (b) after adsorption.

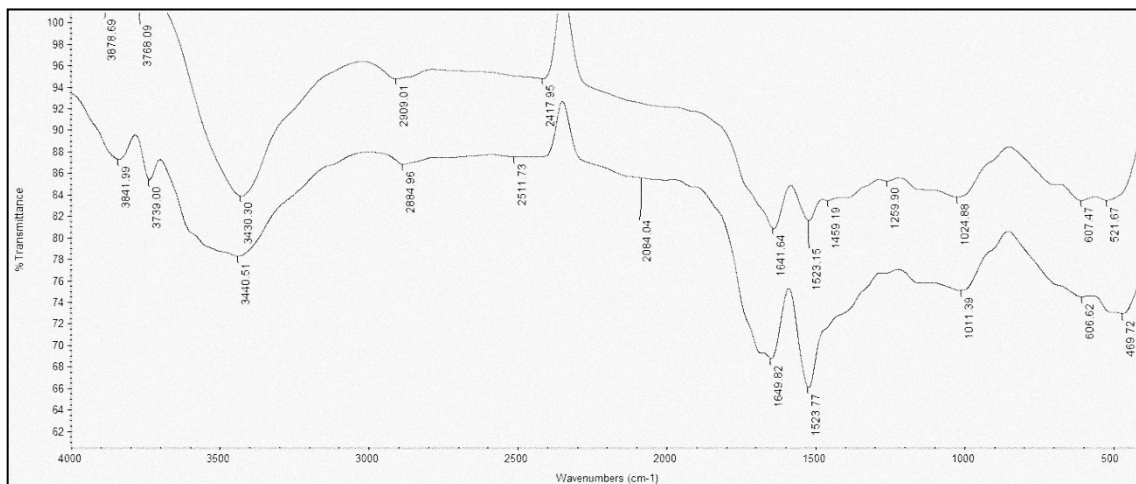


Fig. 1.b. FTIR spectra for MRS (a) before and (b) after adsorption.

### 3.1.3. Scanning electron (SEM) micrographs

Fig. 2 show the SEM micrographs of the RS and MRS before and after loading. The studies demonstrate the presence of hollow cavities with irregular surfaces and many micropores in the periphery of the adsorbents activated. Micrographs show considerable changes in morphology of biosorbent after activation with increased number of cavities on activated surface responsible for more adsorption potential of MRS.

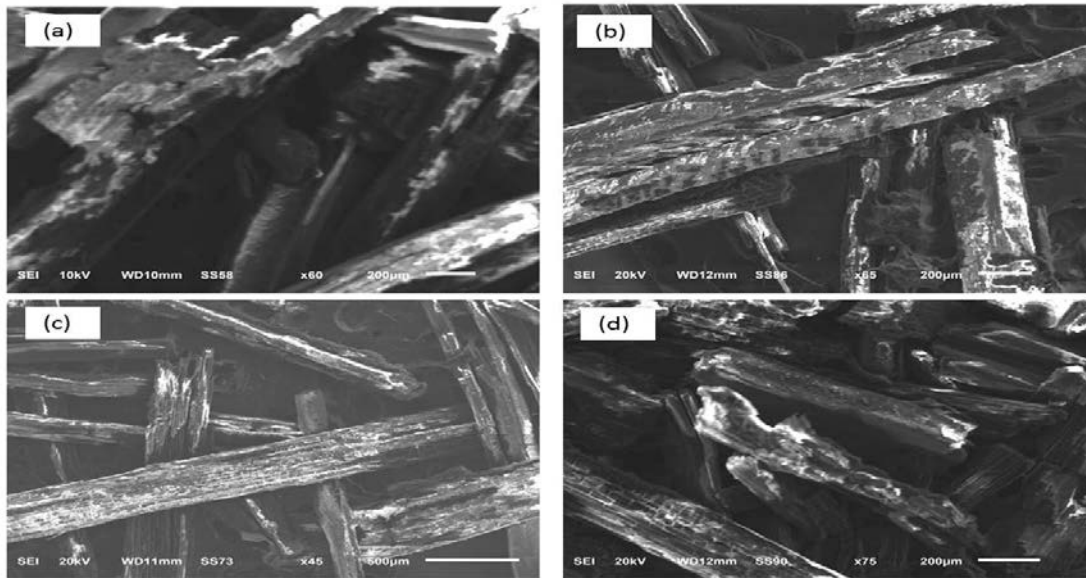


Fig. 2. SEM for (a) RS and (b) MRS before adsorption and for (c) RS and (d) MRS after adsorption.

### 3.1.4. EDXA Spectra

Scanning electron (SEM) micrographs of untreated (RS) and treated rice straws (MRS) are shown in (Fig. 3) and its possible change following Co(II) uptake. In comparison to the EDX spectrums the unloaded MRS did not show the characteristic signal of cobalt metal, whereas the EDX pattern for the cobalt loaded MRS revealed distinctive two peaks for the metal ion. Therefore, the existence of the metal on the RS and MRS surface after adsorption was confirmed by EDX spectra.

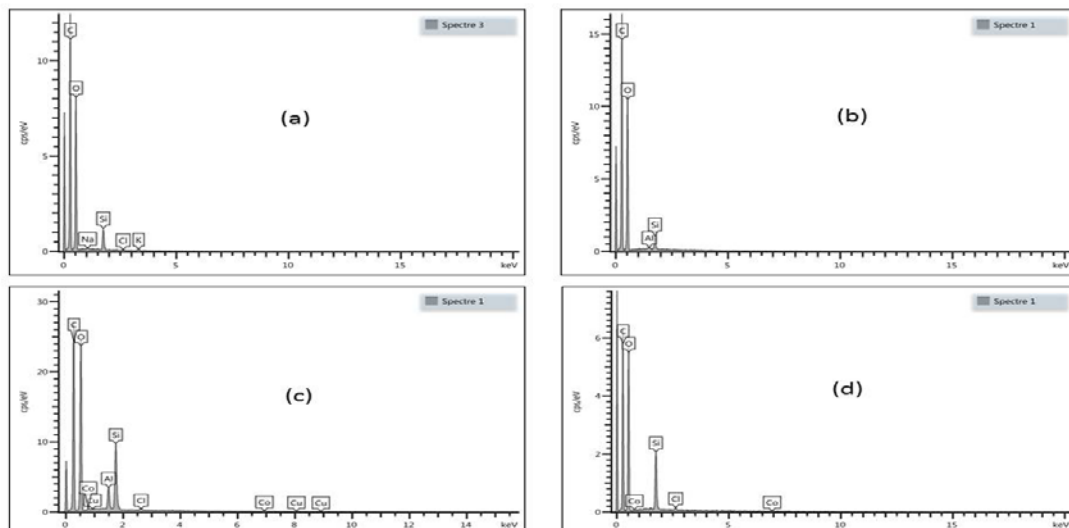


Fig. 3. EDXA for (a) RS and (b) MRS before adsorption and for (c) RS and (d) MRS after adsorption.

### 3.1.5. X-ray diffraction (XRD)

Cellulose has crystalline structure contrary to hemicellulose and lignin, which are amorphous in nature. According to Zhang [10], cellulose has a crystalline structure due to hydrogen bonding interactions and Van der Waals forces between adjacent molecules. X-ray diffraction (XRD) analysis was completed to evaluate the crystallinity of the rice straw after different chemical treatment stages as shown in (fig 4). Chemical treatment performed on natural fibers can affect the crystallinity of cellulose. For example, dilute acid (HCl) has no effect on the crystalline domains, but destroys the amorphous region of the fiber [11,12].

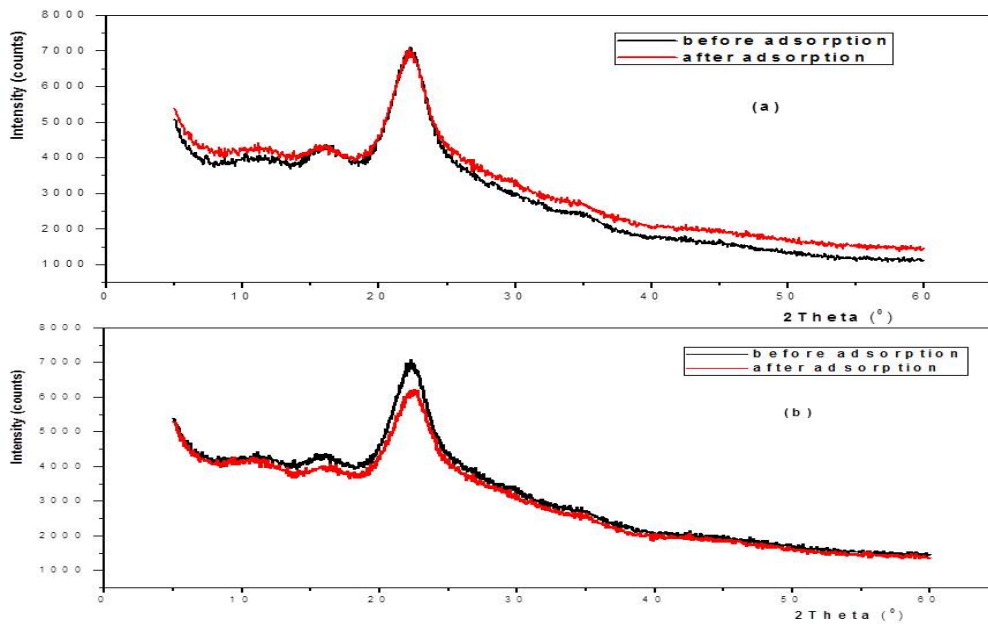


Fig.4 XRD for (a) RS and (b) MRS before adsorption and after adsorption.

### 3.2. Effect of solution pH values

The study of pH has pronounced effects on sorption, so it was studied over the range 1.8–7.1 at prior mentioned conditions. For cobalt, the adsorption pH (1.8–7.1 ± 0.1) was chosen to avoid the precipitation of the metal hydroxides.

At pH 1.8 and 3.1, the uptake capacity of acid pretreated RS biomass for Co(II) was very low due to extreme competition between hydrogen and metal ions present in the liquid phase. The active binding sites got protonated at low pH resulting in the generation of repulsive forces between metal ion Co(II) and active adsorption sites and thereby decrease the interaction of metal ions with the cells [13], which led to under privileged adsorption of Co(II). With the increase in pH from 4.5 to 6.3, removal of metal ion increased. The increase in pH leads to decrease in repulsive forces and generation of attractive forces between active sites of adsorbent and Co(II). On increasing pH, more ligands (carrying negative charges) would be exposed with the subsequent attraction of positively charged metal ions. The maximum removal of Co(II) with RS and pretreated MRS biomasses across the liquid phase was

obtained at pH 6.3. Above pH 6.3, the hydrolysis of Co(II) starts leading to the formation of the formation of metal–hydrolyzed species  $[M(OH)^+]$  could occur with consequent precipitation of metal–ion hydroxides  $[M(OH)_{2(s)}]$  resulting in weakening of positive charge density, which in turn decreases the uptake capacity of RS and pretreated MRS biomasses [14] and thus making the studies above and below these values (pH 7.1) impracticable as shown in fig. 5. The results revealed that pH has a significant effect on Co(II) binding to pretreated RH biomasses. The equilibrium and kinetics modeling was only applied on the pretreated MRS biomasses with increased uptake capacity compared to non-treated RS.

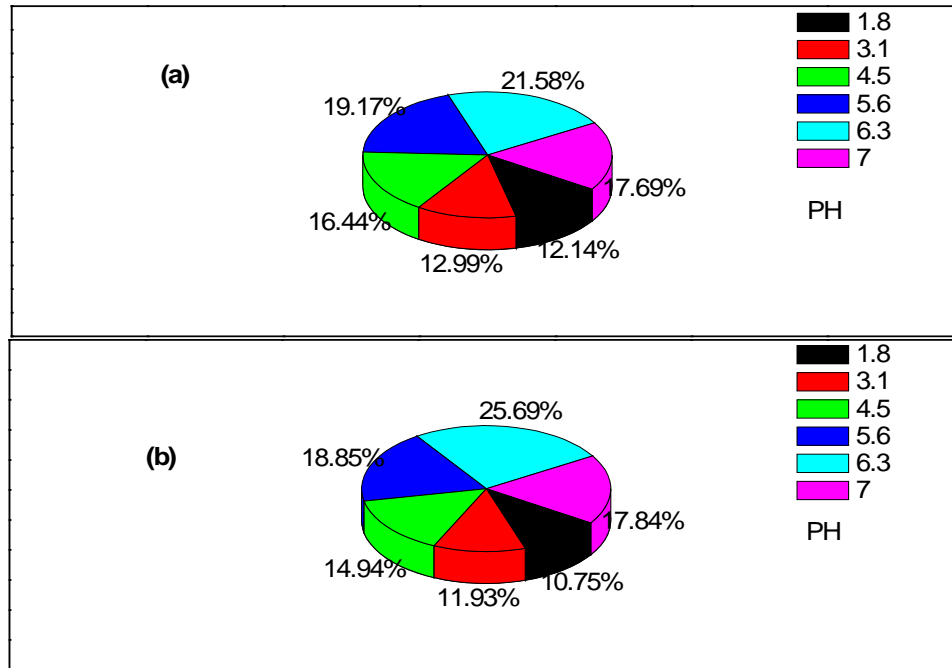


Fig.5. The effect of PH on the removal of co(II) using (a) RS and (b) MRS.

### 3.3. Sorbate concentration

The effect of sorbate concentration on the removal efficiency of sorbent was monitored over the concentration ranges; Co(II) (117.86 - 825.05 mg/l) solutions on its own uptake by 0.4 g of RS and MRS using selected optimized conditions. The uptake rate of the cobalt ion Co(II) increases along with increasing the initial cobalt concentration, if the amount of biomass is kept unchanged. Contrary to that, uptake capacity of the metal ions is inversely proportional to the amount of the biomass when the initial concentration of metal ions is kept constant. A corresponding decrease in removal percentage with the increase in concentration of sorbate was observed, illustrating that at higher concentration of sorbates, limited number of sorption sites are available onto sorbent surface and the study is in agreement with earlier reported work [15] as shown in fig. 6.

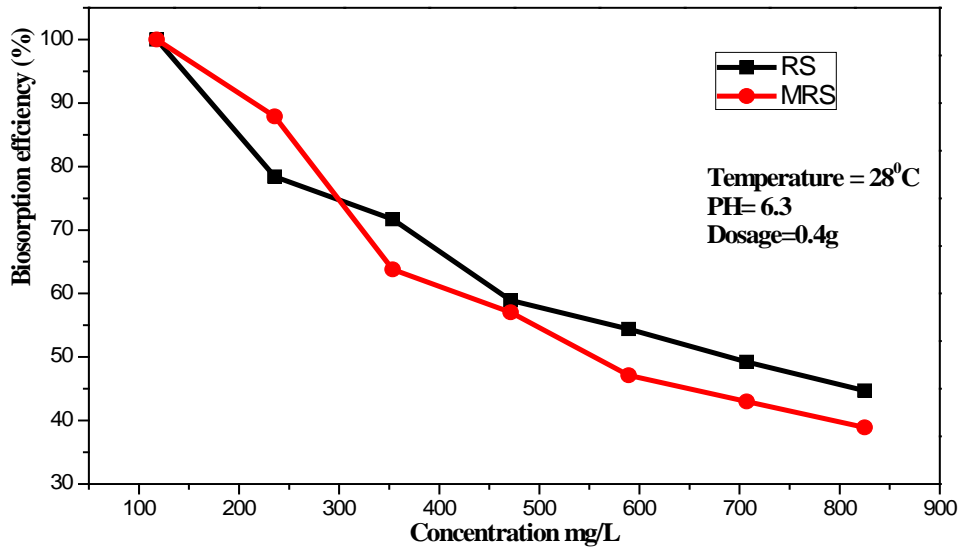


Fig.6. The effect of concentration on the removal of Co(II) onto RS and MRS.

### 3.4. The distribution ratio (D)

Distribution ratio D for cobalt ions was determined by the batch method at different temperature systems (301, 313 and 323K). The distribution ratio, D, is defined as the ratio of metal ion concentration on the adsorbent to that in the aqueous solution and can be used as a valuable tool to study Co(II) ion mobility. The distribution ratio D is defined by the following relationship:

$$K_d = \frac{(I-F)}{500 \text{ mg}} \times \frac{50 \text{ ml}}{F}$$

Where I is the volume of EDTA used before treatment of metal ion-exchange. F is the volume of EDTA consumed by metal ion left in solution phase. Fig. 7 shows that the distribution ratio (D) values increase with the increase in temperatures of cobalt solutions. A corresponding increase in distribution coefficient ( $K_d$ ) with the increase in temperature of sorbate solution was observed, illustrating that at higher temperature of sorbates, large number of sorption sites are available onto sorbent surface and the study is in agreement with earlier reported work [16,17]. The rapid metal sorption has significant practical importance, as this will facilitate with the small amount of adsorbent to ensure efficiency and economy.

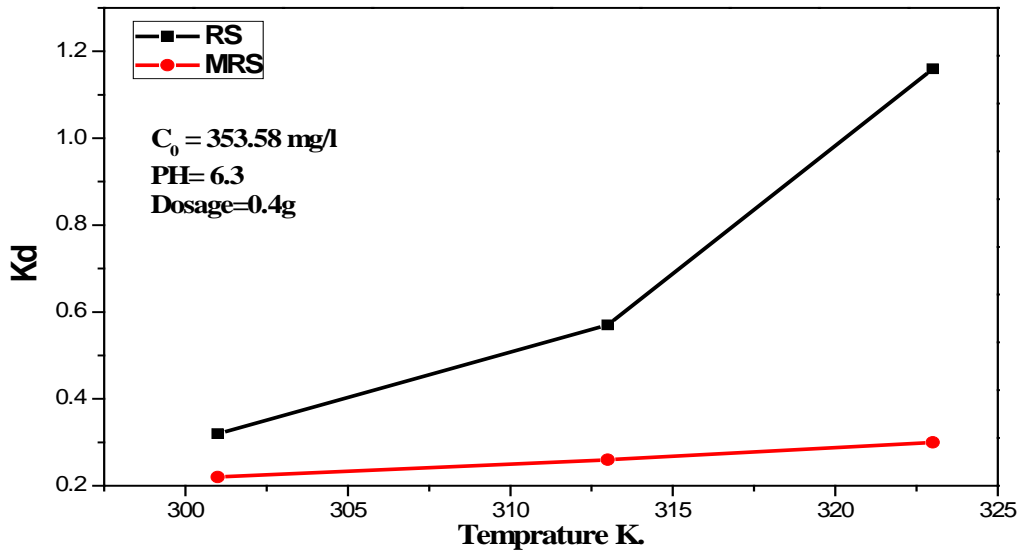


Fig. 7. The effect of distribution coefficient on adsorption of Co (II) by RS and MRS

### 3.5. Effect of the ionic strength

Perusal of (Figs. not shown) clearly demonstrate that the presence of electrolyte in the reacting medium plays a relevant role, particularly the progressive increase of the electrolyte concentration in solution leads to a drastic reduction of the Co (II) uptake by RS and MRS adsorbents.

The influence of the ionic strength on the capacity of cobalt adsorption on the two adsorbents in the presence of different electrolyte in various concentrations media has been tested with the addition of NaCl, NaNO<sub>3</sub> and Na<sub>2</sub>SO<sub>4</sub> to the cobalt solution. The increase in ionic strength between 0.001 and 0.1 has decreased the percentage of adsorption in cobalt-electrolyte-RS and -MRS systems. This may be due to the following two reasons: I) The electrostatic attraction seems to be a significant mechanism, as indicated by the results where, in high ionic strength, the increased amount of the electrolyte can help to render the surface of the rice straw not easily accessible to cobalt (II) ions and hence decreasing the absorption rate. In fact, according to the Surface Chemistry Theory developed by Guoy and Chapman [18], when solid adsorbent is in contact with sorbate species in solution, they are bound to be surrounded by an electrical diffused double layer, the thickness of which is significantly expanded by the presence of electrolyte. Such expansion inhibits the adsorbent particles and Co (II) from approaching. b) The relative competition between sodium ions and cobalt species for the active sites of rice straw can also be an explaining factor. However, the thickness of the electrical diffused double layer was found to be NaCl < NaNO<sub>3</sub> < Na<sub>2</sub>SO<sub>4</sub> Thus, the order of cobalt uptake by the RS and MRS in different electrolyte systems was NaCl > NaNO<sub>3</sub> > Na<sub>2</sub>SO<sub>4</sub> solutions. A similar trend has been observed by earlier investigators [19,20].

### 3.6. Amount of adsorbent

Increase of the biomass concentration of the biosorption system could result in increasing the sorption site interactions for RS and MRS. When the biomass concentration is low, metal ions Co(II) in the solution would not only be adsorbed to surface of the biomass, but also enter into intracellular part through facilitating the concentration gradient of cobalt ion. Results revealed that adsorption capacity ( $q_e$ ) increased with increase of initial c ion cobalt concentration due to the increase of the availability of the metal ions in a fixed biosorbent dose (Fig. 8). This sorption characteristic represented that surface saturation was dependent on the initial Co(II) concentrations. As a matter of fact, biosorption capacity of metal ions reported was related to the ratio of the concentration of initial cobalt ions to the concentration of biomass [21].

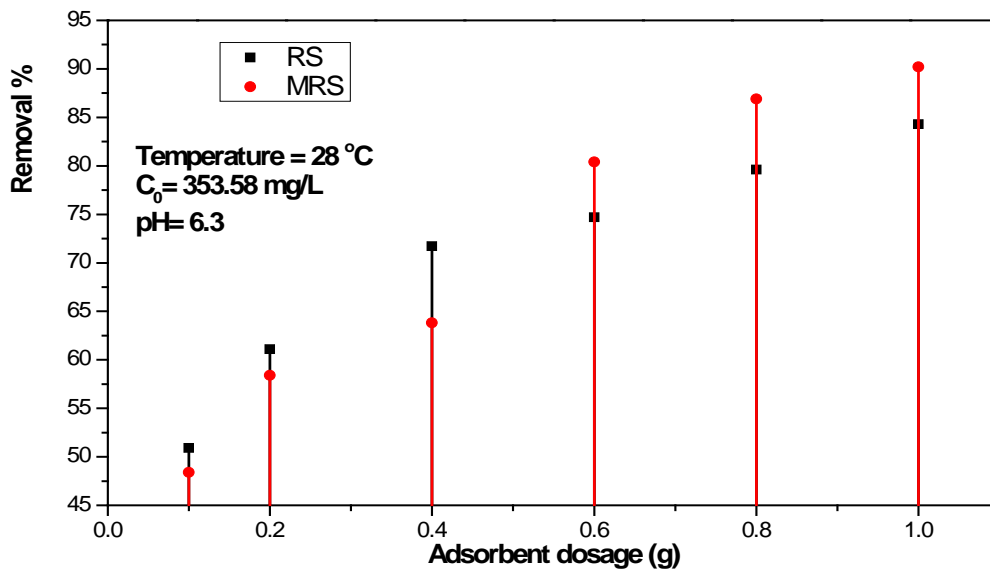


fig.8. Effect of amount of adsorbent on the removal of Co (II) onto RS and MRS

### 3.7. Biosorption Isotherms

Analysis of biosorption data is necessary for the development of biosorption isotherms, biosorption kinetics, and thermodynamic models. These models are used for optimization of design parameters. The interaction between biosorbent and sorbate can be determined by the biosorption isotherm models, namely, Freundlich [22], Langmuir [23], Dubinin–Radushkevich (D–R) [24] and Temkin [25] models at different temperatures.

#### Freundlich isotherm

The Freundlich isotherm is the earliest known equation explaining the biosorption mechanism (Freundlich, 1906). This model is based on the assumption that the biosorption process takes place by the interaction of the sorbate on the heterogeneous surfaces. There is a logarithmic decline in the energy of biosorption with the increase in the occupied binding sites. In addition, Freundlich isotherm

presumes the uptake of sorbate on a heterogeneous surface by multilayer sorption and may be tested using the linearized form of equation (1) as:

$$\log q_e = \log K_F + \frac{1}{n} \log C_e \text{ ----- 1}$$

where  $q_e$  (mg/g) and  $C_e$  (mg/l) are sorbed and equilibrium concentrations of sorbate onto sorbent surface and in solution at equilibrium,  $k_F$  (mg/g) represents the multilayer sorption capacity of sorbent and  $n$  is a characteristic constant measure of intensity of sorption and estimated from the intercept of the linear plots. The values of  $n$  computed from the slope of the plots (2.2) indicate better sorption of sorbate along of temperatures and the results of  $k_F$  (251.1) although, the value of correlation coefficients showed that the Freundlich model (0.90731) was poor fitted for HCl-treated biomass as in [table 2](#).

Langmuir isotherm

The Langmuir adsorption isotherm (Langmuir, 2000) is frequently applied for the biosorption of organic and inorganic pollutants (dyes and heavy metals) from aqueous solution. This model suggests that the biosorption into the adsorbent surface is homogeneous in nature. According to Langmuir isotherm, the biosorption of solute from aqueous solution onto the biosorbent surface is occurring as monolayer biosorption on the homogeneous number of exchanging sites. This phenomenon describes the uniform biosorption energy on the biosorbent surface. The help of linearized form of relationship in equation (2) as:

$$\frac{C_e}{q_e} = \frac{1}{K_L Q_{max}} + \frac{C_e}{Q_{max}} \text{ ----- 2}$$

where ‘ $b$ ’ is the Langmuir constant ( $L \text{ mol}^{-1}$ ) and  $C_o$  is the initial concentration of sorbate (mg/l). In linear Plots of  $C_e/q_e$  versus  $C_e$ , the values of  $Q_{max}$  (mg/g) are analyzed from the slope of the linear plots and the results are enlisted in [table 2](#), whereas the values of ‘ $b$ ’ (0.026 for Co(II)) are computed from the intercepts of the plots.

The important features of the Langmuir isotherm model can be defined by the dimensionless constant separation factor  $R_L$ , which is expressed by the following equation (3) as:

$$R_L = 1 / (1 + K_L C_o) \text{ ----- 3}$$

A dimensionless constant, separation factor,  $R_L$  [26] describes the type ( $R_L = 0$  irreversible,  $R_L = 0 < R_L > 1$  favorable and unfavorable  $R_L > 1$ ) of Langmuir isotherm, which is an essential characteristic of Langmuir isotherm and calculated in the temperature range (301 - 323K).

The values of  $R_L$  in the range (0.098) assign a highly favorable sorption of Co ion solutions. The value of correlation coefficients showed that the Langmuir model was the best fitted for HCl-treated biomass (0.99885) in comparison with Freundlich model (0.90731).

Dubinin–Radushkevich (D–R) isotherm

Dubinin–Radushkevich isotherm assumes a fixed volume or ‘sorption space’ close to the sorbent surface and determines the heterogeneity of sorption energies within the sorption space and is applied in the linearized form of the equation as (4),

$$\ln q_e = \ln X_m - \beta \epsilon^2 \text{ ----- 4}$$

where  $q_e$  is in mg/g (described earlier),  $X_m$  represents the maximum sorption capacity of sorbent (mg/g) and  $\beta$  ( $\text{kJ}^2 \text{mol}^{-2}$ ) is a constant with dimensions of energy. The Polanyi sorption potential  $\epsilon$ , which is the amount of energy required to pull a sorbed molecule from its sorption site to infinity may be evaluated by using relationship

where ‘R’ is a gas constant in  $\text{J mol}^{-1} \text{K}^{-1}$ , ‘T’ is the temperature in Kelvin,  $C_e$  (mg/l) is as mentioned earlier. The plots of  $\ln q_e$  versus  $\epsilon^2$  yield coefficients of determinations 0.96419 and the result of  $X_m$  (24.6) computed from the slope and intercept of respective plots are documented in **table 2**.  $R^2$  values (0.96419) showed that the D–R model poor fit to the experimental data.

The mean free energy of biosorption (E) can be defined as the free energy change when one mole of ion is transferred from infinity in solution to the biosorbent [27]. It can be calculated using the relationship equation (5) as:

$$E = 1/\sqrt{-2B} \text{ ----- 5}$$

The E value in our studies shows a high value ( $116.2 \text{ kJ mol}^{-1}$ ), indicating the chemical nature of the cobalt adsorption processes onto acid treated MRS.

Temkin Isotherm

The Temkin isotherm model (Temkin and Pyzhev, 1940) suggests an equal distribution of binding energies over the number of the exchanging sites on the surface. The distribution of these energies depends on the nature of adsorbate species and the biosorbent surface. The decline in the heat of adsorption is linear, but not logarithmic in nature [28]. The linear form of Temkin isotherm can be written as in equation (6):

$$q_e = B_T \ln A_T + B_T \ln C_e \text{ ----- 6}$$

where  $B_T = RT/b$ , T is the absolute temperature in Kelvin and R is the universal gas constant ( $8.314 \text{ J/mol/K}$ ),  $A_t$  is the equilibrium binding constant and  $B_T$  is corresponding to the heat of sorption. The results of the isotherm parameters/constants are given in **tables 2**. The correlation coefficients for HCl

treated biomass were high (0.99655) and showed good linearity. So, it can be said that the experimental data of cobalt were also better fit to the Temkin isotherm model.

Table 2 : Adsorption isotherm parameters for (353.58 mg/L) of Co(II) on RS and MRS in aqueous solution.

Rice Straw	Langmuir parameters				Freundlich parameters		
	Q <sub>o</sub> (mg/g)	b (L/mg)	R <sub>L</sub>	R <sup>2</sup>	n	K <sub>f</sub> (mg/g)	R <sup>2</sup>
RS	28.5	0.009	0.24	0.99240	4.7	86.1	0.92857
MRS	19.8	0.026	0.098	0.99885	2.2	251.2	0.90731
Rice Straw	D – R parameters				Temkin parameters		
	β	X <sub>m</sub> (mg/g)	E kJ/mol	R <sup>2</sup>	K <sub>t</sub> (L/g)	B <sub>t</sub> (J/mol)	R <sup>2</sup>
RS	3.7x10 <sup>-5</sup>	32.4	116.2	0.67008	1.5x10 <sup>-4</sup>	7.62	0.95294
MRS	3.7x10 <sup>-5</sup>	24.6	116.2	0.96419	1.1x10 <sup>-3</sup>	14.5	0.99655

### 3.8. Biosorption Kinetic Models

The experiments were conducted to determine the time required for MRS biomasses to bind Co(II). The Co(II) uptake was rapid within first 30 min followed by slow sorption till equilibrium was reached. From this sorption behavior of MRS biomasses; it can be concluded that Co(II) uptake by MRS biomasses followed a two steps mechanism, where the metal ion was chemically taken up onto the surface of the biosorbent before being taken up into the inner adsorption sites of dead cells [21]. The first step, known as a passive surface transport, took place quite rapidly, i.e. within 30 min, while the second passive diffusion step transport, could take much longer time to complete. The fast metal uptake (within first 30 min) observed is of particular importance to process design and operation in practical uses. The mechanism of biosorption such as mass transport and chemical reaction procedures must be investigated to fully understand adsorption kinetics. When the biomass is employed as a free suspension in a well-agitated batch system, the effect of external film diffusion on biosorption rate can be assumed not significant and ignored in any kinetic analysis.

Kinetic studies are necessary to optimize different operating conditions for the biosorption. The rate of biosorption process depends on the physical and chemical properties of the biosorbent material and the mass transfer mechanism. The kinetics of cobalt onto the treated rice straw was analyzed using pseudo-first-order [29], pseudo-second-order [30], and intraparticle diffusion [31] kinetic models. The applicability of these kinetic models was determined by measuring the correlation coefficients (R<sup>2</sup>).

Pseudo-First-Order Kinetic Model

Pseudo-first-order kinetic model is based on the fact that the change in cobalt solution temperature with respect to time is proportional to the power one. The linearized equation is described as follows (7) :

$$\log(q_e - q_t) = \log q_{e,1} - k_1 t \text{ ----- } 7$$

where  $q_e$  and  $q_t$  are the biosorption capacity (mg/g) at equilibrium and time  $t$ , respectively,  $k_1$  is the rate constant ( $L \text{ min}^{-1}$ ) of pseudo-first-order kinetic model.

The values of rate constant  $k_1$ ,  $q_e$  calculated,  $q_e$  experimental, and  $R^2$  of cobalt is presented in **tables 3**. In linear plots of  $\ln (q_e - q_t)$  versus  $t$ , the values of  $k$  (0.018, 0.019 and 0.023 for Co ions at three temperatures, 301, 313 and 323K, respectively) are computed from the slopes of the corresponding plots. The results showed that the  $q_e$  calculated is not equal to  $q_e$  experimental and the values of  $R^2$  values of cobalt with HCl treated biomass are not satisfactory. Mostly, the first-order kinetic model is not fitted well for whole data range of contact time and can be applied to the preliminary stage of the biosorption mechanism (Aksu and Donmez, 2003). This suggested that the biosorption of cobalt is not likely to follow the first order kinetic model.

Pseudo-Second-Order Kinetic Model

The biosorption mechanism over a complete range of the contact time is explained by the pseudo-second-order kinetic model as shown below equ.(7,8):

$$\frac{t}{q_t} = \frac{1}{k_2 q_{e,2}^2} + \frac{t}{q_{e,2}} \text{ ----- } 7$$

$$h = k_2 q_{e,2}^2 \text{ ----- } 8$$

where  $k_2$  (g/mg/min) is the second order rate constant of the biosorption process. The second-order parameters  $k_2$ ,  $q_e$  calculated,  $q_e$  experimental, and  $R_2$  of cobalt is shown in **tables 3**. The values of  $q_e$  calculated and  $q_e$  experimental for cobalt are quite same. The correlation coefficients ( $R^2$ ) for HCl-treated biomass for cobalt are also very high (0.99841) which showed that the pseudo second-order kinetic model good fit to kinetic data. The results predicted that the effectiveness, suitability, and applicability of pseudo-second-order kinetic model was more than pseudo-first order kinetic model. When the temperature was increased, the initial adsorption rate  $h$  (mmol/(g min)) of cobalt onto MRS also increased.

Intraparticle Diffusion Model

The movement of cobalt ions (adsorbate) from aqueous solution to the biosorbent surface takes place through various steps. In the first step called bulk diffusion, the transportation of cobalt ions to the solid

biosorbent phase takes place. The second step involves the boundary layer diffusion of adsorbate molecules on the biosorbent surface which is called film diffusion. In the third step called pore or intraparticle diffusion, the cobalt ions move from the outer surface of biosorbent into the internal pores. The fourth step involves a chemical reaction in which the cobalt ions are adsorbed onto the active binding sites of the biosorbent material. The biosorption mechanism may be controlled by a single step or combination of many steps. In a batch experiment system which involves fast and continues stirring, there is a possibility that the intraparticle diffusion is only the rate determining or rate controlling step. The intraparticle diffusion equation is written as follows equ.(9):

$$q_t = K_p t^{1/2} + C \text{ ----- 9}$$

where C is the intercept which describes the boundary layer thickness and  $K_p$  ( $\text{mg/g min}^{1/2}$ ) is the rate constant of intraparticle diffusion. The values of  $K_p$  and C for cobalt are given in tables 3. The intraparticle diffusion played important role in the biosorption process, if the plot of  $q_t$  versus  $t^{1/2}$  passes through the origin. But the lines were not passed through the origin and values of correlation coefficient are also low. Thus the results showed that the biosorption of cobalt onto the treated rice straw does not only depend on intraparticle diffusion, but many other mechanisms may be involved [32]. Therefore, the data are not fitted well to the intraparticle diffusion model. The value of intercept C decreased with an increase in the cobalt solution temperature showing the decrease in boundary layer thickness.

Table 3 : Kinetic parameters for (353.58 mg/L) of Co(II) on RS and MRS in aqueous solution.

Rice Straw	Temp.K	Pseudo first-order model			Pseudo second-order model				Intraparticle diffusion model		
		$q_{e,1,cal}$ (mg/g)	$K_1$ ( $\text{min}^{-1}$ )	$R^2$	$q_{e,2,cal}$ (mg/g)	$K_2$ (g/mg min)	h (mg/g min)	$R^2$	$K_{int}$ $\text{mg/g min}^{-0.5}$	C (mg/g)	$R^2$
RS	301	13.14	0.018	0.99145	32.41	$4.0 \times 10^{-3}$	4.2	0.99959	0.759	19.779	0.85229
	313	19.83	0.023	0.94626	37.20	$3.3 \times 10^{-3}$	4.6	0.99916	1.092	20.432	0.88023
	323	20.94	0.024	0.98666	41.05	$3.1 \times 10^{-3}$	5.2	0.99947	1.261	21.951	0.84888
MRS	301	12.72	0.018	0.95044	28.84	$4.2 \times 10^{-3}$	3.5	0.99841	0.741	17.197	0.9356
	313	14.54	0.019	0.9552	31.00	$2.6 \times 10^{-3}$	2.5	0.99156	0.837	17.516	0.93365
	323	17.05	0.023	0.95495	32.02	$3.6 \times 10^{-3}$	3.7	0.99875	0.908	17.891	0.91301

### 3.9. Influence of temperature

Temperature mainly influences metal ion adsorption by affecting the chemical structure of an adsorbent surface, as well as the physical and chemical status of a solution. Temperature influences the rate of ion movement in a solution, which affects ion adsorption and desorption. Therefore, controlling the appropriate adsorption temperature is necessary for an adsorbent to achieve the optimal adsorption effect. Ion movement in the solution accelerated as the temperature increased from (301°C to 323°C) in Fig. 9. This acceleration facilitated the exchange of unsaturated ions in the MRS with Co(II), which

benefited the chelation of carboxyl and hydroxyl on the MRS with Co(II). Therefore, cobalt adsorption increased [33].

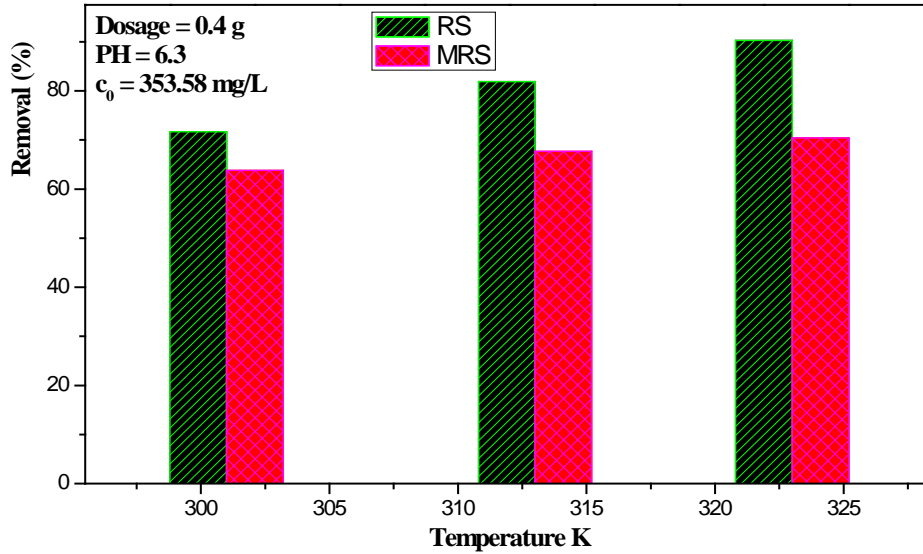


Fig.8. The effect of temperature on the removal of co(II) using RS and MRS.

### 3.10. Thermodynamics of sorption

Thermodynamic parameters, enthalpy  $\Delta H$  ( $\text{kJ mol}^{-1}$ ), entropy  $\Delta S$  ( $\text{J mol}^{-1} \text{K}^{-1}$ ) and standard free energy of activation  $\Delta G$  ( $\text{kJ mol}^{-1}$ ) were investigated in the range of 301–323 K under the optimized conditions chosen by applying the equations(9,10):

$$\log K_d = \frac{\Delta S}{2.301R} - \frac{\Delta H}{2.301RT} \text{ ----- 8}$$

$$\Delta G = \Delta H - T\Delta S \text{ ----- 9}$$

Where ‘R’ is a gas constant, ‘T’ is the temperature in Kelvin. The plots of  $\ln K_d$  versus  $1/T$  ( $\text{K}^{-1}$ ) are linear throughout the investigation and the values of  $\Delta H$  and  $\Delta S$  are computed from the respective slope and intercepts of the plots. The positive values of  $\Delta H$  ( $12.45 \text{ kJ mol}^{-1}$ ),  $\Delta S$  ( $28.53 \text{ J mol}^{-1} \text{K}^{-1}$ ) and  $\Delta G$  ( $-8.6, -8.9$  and  $-9.2 \text{ kJ mol}^{-1}$ ) demonstrate the endothermic, unstable and spontaneous nature of the sorption process, respectively [34].

In order to further support the assertion that the adsorption is the predominant mechanism, the values of the activation energy  $E_a$  8.33 KJ/mol and sticking probability ( $S^*$ ) were estimated from the experimental data and tabulated in table 4. They were calculated using a modified Arrhenius type equation related to surface coverage as expressed in equations (11,12):

$$\theta = 1 - \frac{C_e}{C_0} \text{ ----- 11}$$

$$S^* = (1 - \theta) \exp\left(-\frac{E_a}{RT}\right) \text{ ----- 12}$$

The sticking probability,  $S^*$ , is a function of the adsorbate/adsorbent system under consideration and is dependent on the temperature of the system. The parameter  $S^*$  indicates the measure of the potential of an adsorbate to remain on the adsorbent indefinitely.

The effect of temperature on the sticking probability was evaluated throughout the temperature range from 301 to 323 K by calculating the surface coverage at the various temperatures. Table 4 also indicated that the values of  $S^* \leq 1$  (0.013), hence the sticking probability of the Co(II) ion the adsorbent system are very high.

The apparent activation energy ( $E_a$ ) and the sticking probability ( $S^*$ ) are estimated from the plot (Fig. not shown). These results are indicating that the adsorption processes has a low potential barrier. The positive values of the apparent activation energy  $E_a$  also indicated that the higher solution temperature favors the adsorption process and also the adsorption process is endothermic in nature [35].

Table : 4 Thermodynamic parameters for (353.58 mg/L) of Co(II) on RS and MRS in aqueous solution.

Rice Straw	Temp.K	$\Delta G$ (kJ/mol)	$\Delta S$ (J/mol k)	$\Delta H$ (KJ/mol)	$S^*$	$E_a$ (KJ/mol)
RS	301	-50.2	167.0	53.61	$7.19 \times 10^{-9}$	44.13
	313	-52.2	-	-	-	-
	323	-53.9	-	-	-	-
MRS	301	-8.6	28.53	12.45	0.013	8.33
	313	-8.9	-	-	-	-
	323	-9.2	-	-	-	-

## CONCLUSIONS

The adsorption properties of  $Co^{2+}$  by untreated rice straw and acid treated rice straw were examined in this experiment. The results obtained from the present investigation reveal that:

- The rice straw which is abundantly available and can be easily converted into good adsorbent by using simple method of activation, such as activation with acid.
- Rice straw is an environmentally friendly potential adsorbent for toxic metals. This work examined the efficiency of this adsorbent in removal of some metal ions Co(II) from aqueous and inorganic solution. The present investigation shows that the rice straw is an effective and inexpensive adsorbent for the removal of Co(II).
- It was found that the percentage removal (%) of toxic cobalt ions was dependent on the dose of low cost adsorbent and adsorbent concentration.
- The contact time necessary for maximum adsorption was found to be 4.5 hours.
- The maximum removal of Co(II) with un treated and pretreated RS biomasses was obtained at pH 6.3

## References

- [1] K.J. Zeitsch. *The Chemistry and Technology of Furfural and its Many By-products*, Sugar Series. 2000;31 Elsevier, New York.
- [2] J.Li, G.Henriksson, G. Gellerstedt. Lignin depolymerization and its critical role for delignification of aspen wood by steam explosion, *Bioresour. Technol* 98,2007, 3061–3068.
- [3] N.Mosier, C.Wyman, B.Dale, R.Elander, Y.Y.Lee, M.Holtzapple, M. Ladisch. Features of promising technologies for pretreatment of lignocellulosic biomass, *Bioresour. Technol.* 95, 2005, 673–686.
- [4] C.T Yu., W.H.Chen, L.C.Men, W.S. Hwang. Microscopic structure features changes of rice straw treated by boiled acid solution, *Industrial Crops and Products* 29, 2009, 308-315.
- [5] J.P. Zhu., V.S.O'Dwyer. Chang Granda C.B. structural features affecting biomass enzymatic digestibility, *Bioresour. Technol.* 99, 2008, 3817–3828.
- [6] T.Chieh Hsu , G.Guo , W.Chen, W.g. Hwang . Effect of dilute acid pretreatment of rice straw on structural properties and enzymatic hydrolysis, *Bioresource Technology* 101, 2010, 4907–4913.
- [7] M.Akhtara, S.Iqbal, A.Kausar, M.I. Bhangera, M. Ashraf Shaheen. An economically viable method for the removal of selected divalent metal ions from aqueous solutions using activated rice husk, *Colloids and Surfaces B: Biointerfaces* 75, 2010, 149–155.
- [8] X. Luo, Z. Deng, X. Lin, C. Zhang. Fixed-bed column study for Cu<sup>2+</sup> removal from solution using expanding rice husk, *Journal of Hazardous Materials* 187, 2011, 182–189.
- [9] R. Elangovan, L. Philip, K Chandraraj . Biosorption of chromium species by aquatic weeds: kinetics and mechanism studies, *J. Hazard. Mater.* 152(1), 2008, 100–112.
- [10] Y.P. Zhang, L.R. Lynd *Biotechnol.* Toward an aggregated understanding of enzymatic hydrolysis of cellulose: noncomplexed cellulase systems, *Bioeng.* 88, 2004, 797–824.
- [11] D. Fengel, G. Wegener. *Wood Chemistry, Ultrastructure, Reactions* Walter de Gruyter, Berlin 1984.
- [12] N. Johar, I. Ahmad, A. Dufresne . Extraction, preparation and characterization of cellulose fibres and nanocrystals from rice husk, *Industrial Crops and Products* 37, 2012, 93–99.
- [13] X. Jian Li, C. Jie Yan, W. Jun Luo, Q. Gao, Q. Zhou , C. Liu, S. Zhou . Exceptional cerium (III) adsorption performance of poly (acrylic acid) brushes-decorated attapulgite with abundant and highly accessible binding sites, *Chem. Eng. J.* 284, 2016, 333–342.
- [14] S. Nhandeyara do Carmo Ramos , A. Luísa Pedrosa Xavier, F. Simões Teodoro, L. Frédéric Gil, L. Vinícius Alves Gurgel . Removal of cobalt(II), copper(II), and nickel(II) ions from aqueous solutions using phthalate-functionalized sugarcane bagasse: Mono- and multicomponent adsorption in batch mode, *Industrial Crops and Products* 79, 2016, 116–130.
- [15] Y. Wu, Y. Fan, M. Zhang, Z. Ming, S. Yang, A. Arkin , F. Peng. Functionalized agricultural biomass as a low-cost adsorbent: Utilization of rice straw incorporated with amine groups for the adsorption of Cr(VI) and Ni(II) from single and binary systems, *Biochem. Eng. J.* 105(A), 2016, 27–35

- [16] H. Takata, T. Aono, K. Tagami, S. Uchida. A new approach to evaluate factors controlling elemental sediment–seawater distribution coefficients (Kd) in coastal regions, Japan, *Science of The Total Environment* 543(A), 2016, 315–325
- [17] P. Trinchero, S. Painter, H. Ebrahimi, L. Koskinen, J. Molinero. Modelling radionuclide transport in fractured media with a dynamic update of Kd value, *Jan-Olof Selroos Computers & Geosciences*. 2016;86:55-63
- [18] L. Osipow. *Surface Chemistry: Theory and Industrial Applications*, Krieger, 1972;1 New York.
- [19] S. Cataldo, A. Gianguzza, M. Merli, N. Muratore, D. Piazzese, M. Liria Turco Liveri. Experimental and robust modeling approach for lead (II) uptake by alginate gel beads: Influence of the ionic strength and medium composition, *Journal of Colloid and Interface Sci.* 434, 2014, 77–88.
- [20] L. Jiang, Y. Liu, G. Zeng, F. Xiao, X. Hu, H. Wang, T. Li, L. Zhou, X. Tan. Removal of 17 $\beta$ -estradiol by few-layered graphene oxide nanosheets from aqueous solutions: External influence and adsorption mechanism, *Chemical Engineering Journal* 284, 2016, 93-102.
- [21] M. N. Zafar, Iqra Aslam, Raziya Nadeem, Shahida Munir, Usman Ali Rana, Salah Ud-Din Khan. Characterization of chemically modified biosorbents from rice bran for biosorption of Ni(II); *J. the Taiwan Institute of Chem. Eng.* 46, 2015, 82–88.
- [22] Y. Zhu, N. Gao, Q. Wang, X. Wei. Adsorption of perchlorate from aqueous solutions by anion exchange resins: effects of resin properties and solution chemistry, *Colloids and Surfaces A: Physicochem. Eng. Aspects* 468, 2015, 114–121.
- [23] M. Barnabas, S. Parambadath, A. Mathew, S. Park. Vinu A., Ha C. Highly efficient and selective adsorption of In<sup>3+</sup> on pristine Zn/Al layered double hydroxide (Zn/Al-LDH) from aqueous solutions, *Journal of Solid State Chemistry* 233, 2016, 133–142.
- [24] G. Zhou, J. Luo, C. Liu, L. Chu, J. Ma, Y. Tang, Z. Zeng, S. Luo. A highly efficient polyampholyte hydrogel sorbent based fixed-bed process for heavy metal removal in actual industrial effluent, *Water Research* 89, 2016, 151-160.
- [25] H. Fan, W. Sun, B. Jiang, Q. Wang, D. Li, C. Huang, K. Wang, Z. Zhang, W. Li. Adsorption of antimony(III) from aqueous solution by mercapto-functionalized silica-supported organic–inorganic hybrid sorbent: Mechanism insights, *Chemical Engineering Journal* 286, 2016, 128–138.
- [26] P. Priyabrata, F. Banat. Comparison of heavy metal ions removal from industrial lean amine solvent using ion exchange resins and sand coated with chitosan, *J. Natural Gas Scie. Eng.* 18, 2014, 227-236.

- [27] M.Giorgos, D. Mitrogiannis, A. Celekli, H. Bozkurt, D.Georgakakis, C.V. Chrysikopoulos. Biosorption of Cu 2+ and Ni 2+ by *Arthrospira platensis* with different biochemical compositions, *Chemi. Eng. J.* 259, 2015, 806–813.
- [28] Z. Yongfeng, Z. Yian, W. Ai Qin. A simple approach to fabricate granular adsorbent for adsorption of rare elements, *Internat. J. Biological Macromolecules* 72, 2015, 410–420.
- [29] Z. Ding, X. Hub, Y. Wand, S. Wang, B. Gao. Removal of lead, copper, cadmium, zinc, and nickel from aqueous solutions by alkali-modified biochar: Batch and column tests, *Journal of Industrial and Engineering Chemistry* 33, 2016, 239–245.
- [30] K. Lin, Y. Liu, S. Yi Chen. Adsorption of fluoride to UiO-66-NH<sub>2</sub> in water: stability, kinetic, isotherm and thermodynamic studies *Journal of Colloid and Interface Science* 461, 2016, 79–87.
- [31] M. Seliem, S. Komarneni, M. Abu Khadra. Phosphate removal from solution by composite of MCM-41 silica with rice husk: Kinetic and equilibrium studies, *Microporous and Mesoporous Materials* 224, 2016, 51-57.
- [32] Y. Safa, H. Bhatti, I. Bhatti, M. Asgher. Removal of direct Red-31 and direct Orange-26 by low cost rice husk: Influence of immobilisation and pretreatments, *The canadian journal of chemical engineering* 89, 2011, 1554-1565.
- [33] H. Ren, Z. Gao, D. Wu, J. Jiang, Y. Sun. Efficient Pb (II) removal using sodium alginate–carboxymethyl cellulose gel beads: Preparation, characterization, and adsorption mechanism, *Congwei Luo Carbohydrate Polym.* 137, 2016, 402–409.
- [34] M. Akhtar, S. Iqbal, A. Kausar, M.I. Bhangar, M. Shaheen. An economically viable method for the removal of selected divalent metal ions from aqueous solutions using activated rice husk, *Colloids and Surfaces B: Biointerfaces* 75, 2010, 149–155.
- [35] B. Singh, S. K. Das. Adsorptive removal of Cu(II) from aqueous solution and industrial effluent using natural/agricultural wastes, *Colloids and Surf. B: Biointer.* 107, 2013, 97– 106.